COMPARATIVE ANALYSIS OF MATHEMATICAL MODELS FOR THERMAL STRESS AND DEFORMATION GENERATION IN A SOLIDIFYING INGOT

L. G. Dymova, P. V. Sevast'yanov, and V. I. Timoshpol'skii

UDC 621.746

Using the example of solidification of a plane steel ingot calculated thermal stresses and deformations obtained in the elastic, elastoplastic, and viscoelastic approximations are compared.

Introduction. One of the most important problems in ingot pouring, both in the case of individual parts and in the continuous method, is the determination of technological regimes which will produce parts without voids. Solution of this problem by a purely experimental approach is practically impossible, since voids develop both on the surface and within the casting.

This fact is one of the reasons for the increased interest of researchers in computational methods for determining stresses and deformations in the solidifying ingot.

It is well known that the stressed-deformed state in the casting is determined by the nonsteady state temperature field. At the present time there exist reliable and widely used mathematical models for calculation of nonsteady state heat exchange during casting, which allow prediction of temperature fields with an accuracy sufficient for practical purposes [1, 2].

As for modelling of thermal stresses and deformations specifically, there is at present no one unified approach. Thus, [3] utilized a thermoelastic approximation, [4-6] solved the thermoelastoplastic problem, while [7-9] used a model involving viscoelastic behavior of the material. There also exist a large number of other formulations of the problem within the framework of these basic approaches. The differences between results of calculations with the various models are often quite large. As was shown in [9], the stresses in the early stages of solidification of a steel ingot in continuous casting crystallizers calculated by the thermoelastic model are two orders of magnitude greater than the stresses found in the viscoelastic model. At the same time the relaxation time estimates carried out in [6] indicate the possibility of neglecting viscous effects in this case. The situation is complicated even more by the lack of reliable data on mechanical properties of the materials involved at high temperatures.

As was noted in [8, 9], at present two basic approaches are used most widely for calculating thermal stresses in the ingot, based on models of elastoplastic and viscoelastic behavior of the material involved.

The present study will carry out a comparison of these approaches with each other and with the thermoelastic solution using the simple yet practically important case of solidification of a planar ingot of type 45 steel in a cast iron mold.

To calculate the thermal processes the mathematical model of [2, 5], well recommended by practice, was used for solidification of a planar ingot of thickness $2H_1$ with mold wall thickness H_2, which model with the origin chosen on the ingot axis has the form

$$\rho_1(T_1)\, c_1(T_1) \frac{\partial T_1}{\partial \tau} = \frac{\partial}{\partial x}\left(\lambda_1(T_1) \frac{\partial T_1}{\partial x}\right), \tag{1}$$

$$\rho_2(T_2)\, c_2(T_2) \frac{\partial T_2}{\partial \tau} = \frac{\partial}{\partial x}\left(\lambda_2(T_2) \frac{\partial T_2}{\partial x}\right), \tag{2}$$

$$T_1|_{\tau=0} = T_{01},\ T_2|_{\tau=0} = T_{02},\ \left.\frac{\partial T_1}{\partial x}\right|_{x=0} = 0, \tag{3}$$

Belorussian Polytechnic Institute, Minsk. Translated from Inzhenerno-Fizicheskii Zhurnal, Vol. 60, No. 1, pp. 115-120, January, 1991. Original article submitted October 13, 1989.

0022-0841/91/6001-0099$12.50

$$\lambda_1 \frac{\partial T_1}{\partial x}\Big|_{x=H_1} = -\varkappa_1 (T_1^4 - T_2^4)|_{x=H_1}, \tag{4}$$

$$\lambda_2 \frac{\partial T_2}{\partial x}\Big|_{x=H_1} = -\varkappa_1 (T_1^4 - T_2^4)|_{x=H_1}, \tag{5}$$

$$\lambda_2 \frac{\partial T_2}{\partial x}\Big|_{x=H_1+H_2} = -\varkappa_2 (T_2^4 - T_c^4)|_{x=H_1+H_2} + \alpha (T_2 - T_c)|_{x=H_1+H_2}, \tag{6}$$

$$c_1(T) = \begin{cases} c_s(T), & T < T_S, \\ c_t = c_s - L\dfrac{\partial \psi}{\partial T}, & T_S \leqslant T \leqslant T_L, \\ c_\ell(T), & T > T_L. \end{cases} \tag{7}$$

where the subscript 1 refers to the casting, 2 to the mold.

In accordance with the recommendations of [1] in the liquid portion of the casting we take

$$\lambda_1 (T_1(0, \tau)) = \lambda_\ell (1 + a(T_1(0, \tau) - T_L)^{1/4}). \tag{8}$$

Dependences of the thermophysical properties on temperature were taken from [10], with α and $\varkappa_2$ from [11].

Following [11], in Eqs. (4), (5) we neglect contact thermal conductivity, which may produce a marked contribution to heat exchange only in the initial stage of solidification and has little effect on the dynamics of solidification in ingots of mass greater than 8 ton.

The model described contains the two quite undefined parameters $\varkappa_1$ and a, the values of which depend significantly on the concrete technological conditions. Therefore the model can be refined by parametric identification, which in the given case reduces to finding $\varkappa_1$ and a by minimizing the discrepancy of the mean square deviations of the calculated and measured temperature on the ingot axis and in the mold at a distance of $3 \cdot 10^{-2}$ m from its working surface.

This extremal problem was solved by standard gradient methods. The calculated dynamics of the process up to the moment of complete solidification of the ingot at $H_1 = 0.36$ m, $H_2 = 0.2$ m, $T_{01} = 1850$ K are shown in Fig. 1.

In constructing the mathematical model for calculation of thermal stresses and deformations it was considered that formation of the stressed state occurs under conditions of changing skin thickness over time, complex heat exchange, etc., i.e., according to the terminology of [12], under complex loading conditions. Under such conditions calculation of stresses and deformation in the presence of plastic or viscous effects requires consideration of the loading history. This can be achieved with sufficient accuracy only within the framework of the flow theory of [12], in accordance with which the process is divided into two successive stages and the problem solved in terms of increments to the stresses and deformations during successive changes in loading.

In this case the solidifying portion of the ingot can be considered infinite along the axes y and z of a plate of thickness h, which varies with time and is defined by the current position of the isotherm T_S, which can be found by solution of the thermal problem of Eqs. (1)-(8).

Neglecting external mechanical loads as compared to thermal ones and considering that the plate temperature depends only on coordinate x, in accordance with [12] for any nth stage of loading we obtain

$$\Delta\sigma_y^n(x) = \Delta\sigma_z^n(x), \tag{9}$$

$$\Delta\sigma_x^n = \Delta\sigma_{xy}^n = \Delta\sigma_{xz}^n = \Delta\sigma_{yz}^n = 0. \tag{10}$$

The equilibrium equation for conditions (9), (10) is satisfied identically. The deformation compatibility equations take on the form

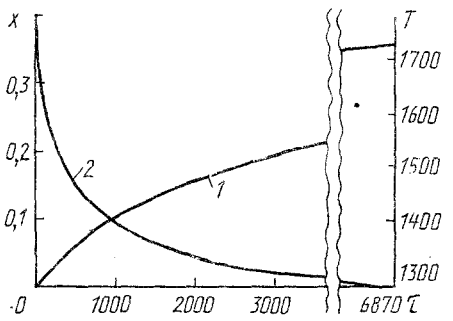

Fig. 1

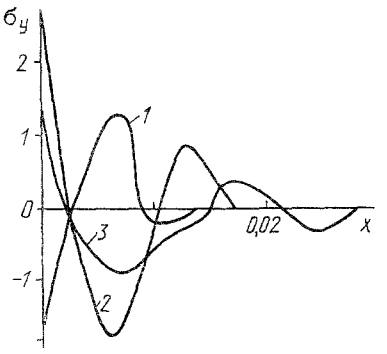

Fig. 2

Fig. 1. Change in thickness of skin (1) and ingot surface temperature (2) during solidification. T, K; x, m; τ, sec.

Fig. 2. Thermoviscoelastic stress dynamics in growing skin: 1) τ = 92 sec; 2) 112; 3) 172.

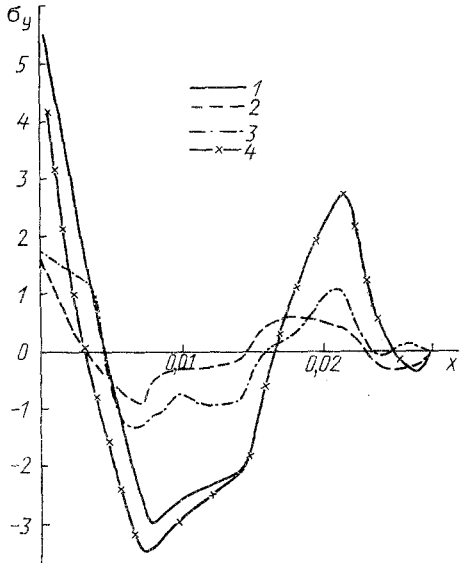

Fig. 3

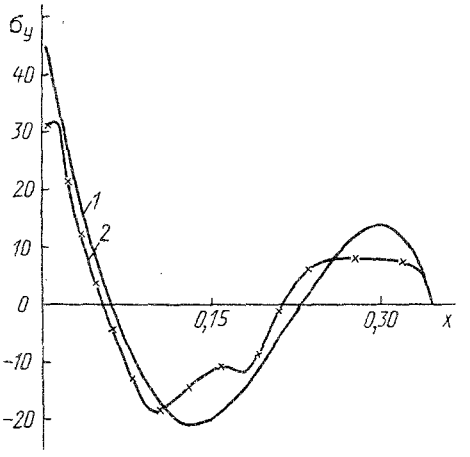

Fig. 4

Fig. 3. Stress distribution over skin thickness at time τ = 170 sec; 1) model of ideal elastic material behavior; 2) viscoelastic material behavior (Maxwell variant); 3) viscoelastic model (Norton variant); 4) elastoplastic model, σ, MPa.

Fig. 4. Stress distribution over skin thickness at moment of complete solidification; 1) ideal elastic model; 2) elastoplastic model.

$$\frac{\partial^2 \Delta\varepsilon_y^n}{\partial x^2} = 0, \quad \frac{\partial^2 \Delta\varepsilon_z^n}{\partial x^2} = 0. \tag{11}$$

The expressions relating the total increments in deformations, as well as their elastic $\Delta\varepsilon^{\ell}$, plastic $\Delta\varepsilon^{p}$, viscous $\Delta\varepsilon^{c}$, and thermal $\Delta\varepsilon^{T}$ components with the stress increments have the form [13] (subscript n omitted for brevity)

$$\Delta\varepsilon_x = \Delta\varepsilon_x^l + \Delta\varepsilon_x^p + \Delta\varepsilon_x^c + \Delta\varepsilon^T, \tag{12}$$

$$\Delta\varepsilon_z = \Delta\varepsilon_y = \Delta\varepsilon_y^l + \Delta\varepsilon_y^p + \Delta\varepsilon_y^c + \Delta\varepsilon^T, \tag{13}$$

$$\Delta\varepsilon_x^l = -\frac{2\mu}{E}\Delta\sigma_y + 2\left(\frac{\mu\sigma_y}{E^2}\frac{dE}{dT} - \frac{\sigma_y}{E}\frac{d\mu}{dT}\right)\Delta T,$$

$$\Delta\varepsilon_y^l = \frac{1-\mu}{E}\Delta\sigma_y - \left(\frac{(1-\mu)\sigma_y}{E^2}\frac{dE}{dT} - \frac{\sigma_y}{E}\frac{d\mu}{dT}\right)\Delta T,$$

$$\Delta\varepsilon_x^p = (F_\sigma(\sigma_i, T)\Delta\sigma_y + F_T(\sigma_i, T)\Delta T)S_x,$$

$$\Delta\varepsilon_y^p = (F_\sigma(\sigma_i, T)\Delta\sigma_y + F_T(\sigma_i, T)\Delta T)S_y, \quad \Delta\varepsilon_x^c = V_x\Delta\tau, \quad \Delta\varepsilon_y^c = V_y\Delta\tau,$$

$$\Delta\varepsilon^T = \alpha_T(T)\Delta T, \quad F_\sigma = \frac{3}{2\sigma_i}\left(\frac{1}{E_k} - \frac{1}{E}\right), \quad F_T = \frac{3}{2\sigma_i}\left(\beta + \frac{\sigma_i}{E}\frac{dE}{dT}\right),$$

$$\sigma_i = \sqrt{(\sigma_y^2 + \sigma_z^2)/2}, \quad S_x = -\frac{2}{3}\sigma_y, \quad S_y = \frac{\sigma_y}{3}.$$

The tangent modulus E_k and the temperature compliance β depend on temperature and the stress intensity σ_i [13] and can be calculated from empirical σ—ε extension diagram. A number of variants of creep theory exist, of which for the present we will consider Maxwell theory, according to which the creep velocity in our case has the form:

$$V_x = \frac{S_x}{2G\tau_p}, \quad V_y = \frac{S_y}{2G\tau_p},$$

and Norton theory:

$$V_x = \frac{3}{2}B(T)\sigma_i^{m(T)-1}S_x, \quad V_y = \frac{3}{2}B(T)\sigma_i^{m(T)-1}S_y.$$

According to [8] the relaxation time of type 45 steel is a function of temperature $\tau_p(T) = 9\cdot10^8\exp(-0.0114\ T)$. The study [9] presented graphs of $B(T)$ and $m(T)$ for a steel close in composition to type 45, which in the temperature range of interest to us can be approximated in the form $m = 5$; $\log B = 0.0117(T - 273) - 21.69$. The problem was solved at each loading step by the method of [14].

It follows from [11] that

$$\Delta\varepsilon_z = \Delta\varepsilon_y = \varepsilon_0 + \varkappa_0 x. \tag{14}$$

The undetermined constants ε_0 and $\varkappa_0$ can be found from the conditions of absence of mechanical stresses and moments

$$\int_0^h \Delta\sigma_y dx = 0, \quad \int_0^h x\Delta\sigma_y dx = 0. \tag{15}$$

In [15] values of $\Delta\sigma_y$ were used found from substitution of Eq. (14) in Eq. (13):

$$\Delta\sigma_y = \frac{\varepsilon_0 + \varkappa_0 x - \Delta\varepsilon^T - \Delta\varepsilon_y^c + \left(\frac{\sigma_y(1-\mu)}{E^2}\frac{dE}{dT} - \frac{\sigma_y}{E}\frac{d\mu}{dT} - F_T S_y\right)\Delta T}{\left(\frac{1-\mu}{E} + \frac{\sigma_y^2 F_\sigma}{3\sigma_i}\right)}. \tag{16}$$

After substitution of Eq. (16) in Eq. (15) the integrals were found numerically. The expanding grid method was used, with the node coordinates changing with time in proportion to the change in skin thickness. As a result at each loading step Eq. (15) provided a system of linear algebraic equations the solution of which provided ε_0 and $\varkappa_0$ and then, using Eq. (16), $\Delta\sigma_y$. Having summed the change in stress thus obtained with the stresses accumulated in previous steps, we find the total stress in the nth loading step: $\sigma_y = \sigma_y + \Delta\sigma_y$, after which we move to the next step.

In performing the calculations the temperature dependence of mechanical properties presented in [9] were used.

Stability of the solution was insured when viscous effects were considered ($\Delta\varepsilon^c \neq 0$) by choice of time steps $\Delta\tau$ less than the characteristic stress relaxation times in the hottest regions of the ingot. A sufficiently precise and stable solution of the elastoplastic problem ($\Delta\varepsilon^c = 0$) can be obtained by satisfying the condition $\Delta T \leq 10$ K for each step in ingot thickness.

Numerical solution was carried out using the temperature fields obtained with the model of Eqs. (1)-(8). The calculated stress fields in the initial stage of ingot formation corresponding to the solidification dynamics shown in Fig. 1 are stages of solidification compressive stresses develop near the cooling surface, their profile corresponding fully with the results of [9] for the case of continuous casting. With further increase in skin thickness the stresses undergo a qualitative change. It follows from Fig. 3 that the solutions obtained in the elastic ($\Delta\varepsilon^p = 0$, $\Delta\varepsilon^c = 0$) and elastoplastic ($\Delta\varepsilon^p \neq 0$, $\Delta\varepsilon^c = 0$) approximations practically coincide. This can be explained by the smallness of the stresses themselves, which exceed the elastic limit only slightly, despite the high temperatures. Consideration of viscous effects significantly decreases the stresses, while solutions obtained with the two viscoelastic material models are quite close to each other, despite the significant difference between the models. Plasticity manifests itself much more significantly in the latter stages of solidification. As is evident from Fig. 4, the elastoplastic approximation yields stresses approximately half as large on the cooling surface than the purely elastic model.

Conclusion. At present there are no experimental data available which permit direct or indirect determination of the adequacy of the models studied for ingot solidification. However it should be noted that despite quantitative divergences, the results of all models studied do agree qualitatively.

The studies performed permit the conclusion that the true stresses in a solidifying ingot lie in a region bounded above by stresses determined by the elastic model, and below by the viscoelastic models. More precise quantitative estimates are apparently impossible at present due to the lack of reliable data on thermophysical and mechanical properties of materials at high temperatures, inhomogeneity of the ingot, and the presence of zones with isometric and columnar crystals.

NOTATION

T_{01}, T_{02}, T_S, T_L, T_c, $T(x, \tau)$ are initial temperatures of melt and mold, temperatures of solidus, liquidus, and surrounding medium, temperature field: ρ, c, λ L, density, specific heat, thermal conductivity, and latent heat of solidification; c_s, c_t, c_ℓ, λ_ℓ, specific heats of solid, two-phase and liquid zones of ingot, thermal conductivity of melt; $\varkappa$, α, radiant and convective heat exchange coefficients; $\Delta\sigma^n$, $\Delta\varepsilon^n$, stress and deformation increments in step n of loading; $\Delta\tau$, time increment; ΔT, temperature increment at point studied within ingot thickness; E, G, μ, moduli of elasticity and shear and Poisson coefficient; α_T, linear expansion coefficient; S_x, S_y, stress deviators; σ, stresses accumulated by step n of loading.

LITERATURE CITED

1. P. F. Balandin, Fundamentals of Casting Formation Theory, Part I [in Russian], Moscow (1976).
2. Yu. A Samoilovich, Systematic Analysis of Ingot Crystallization [in Russian], Kiev (1983).
3. N. I. Nikitenko, N. R. Snovida, D. P. Evteev, and L. A. Sokolov, Thermophysics and Thermotechnology, 30th Ed., [in Russian], Kiev (1976), pp. 43-47.
4. F. H. Weiner and B. A. Boley, J. Mech. Phys. Solids, 11, 145-154 (1963).
5. A. I. Tsaplin and Yu. A. Samoilovich, Continuous Casting of Steel, 3rd Ed. [in Russian], Moscow (1976), pp. 59-65.
6. A. A. Poznyak, Izv. Akad. Nauk. Latv. SSR, Ser. Fiz. Tekh. Nauk, No. 5, 78-82 (1978).
7. L. M. Muradyan, G. G. Nersesyan, G. A. Avetisyan, et al., Engineering Problems in Structural Mechanics [in Russian], Erevan (1985), pp. 63-71.
8. Yu. A. Samoilovich and Z. K. Kabakov, Combustion, Heat Exchange, and Heating of Metal, 24th Ed. [in Russian], Moscow (1973), pp. 100-117.
9. J. O. Kristiansson, J. Thermal Stresses, 5, 315-330 (1982).
10. L. A. Brovkin and S. I. Devochkina, Izv. Vyssh. Uchebn. Zaved., Chern. Metall., No. 3, 164-168 (1978).
11. L. Shmrga, Solidification and Crystallization of Steel Ingots [in Russian], Moscow (1985).
12. Yu. N. Shevchenko, Thermal Strength under Variable Loading [in Russian], Kiev (1960).

13. I. A. Birger and B. F. Shorr, Thermal Strength of Machine Parts [in Russian], Moscow (1975).
14. A. D. Kovalenko, Thermoelasticity [in Russian], Kiev (1975).

CONTACT CONDUCTIVITY OF CRYOGENIC HEAT INSULATION MATERIALS

S. B. Mil'man and M. G. Velikanova

UDC 536.21

Results are presented of an experimental investigation by the method of the electrothermal analogy for the contact heat transfer in different kinds of cryogenic thermal insulation and empirical dependences are obtained that permit execution of a qualitative, and in a number of cases, even a quantitative estimate of the contribution of the contact conductivity to the total heat transport through heat insulation.

In principle, the possibility of an experimental study of contact heat conductivity in disperse materials by the method of the electrothermal analogy (ETA) was shown in [1]. This permits investigation of the contact heat conductivity in a pure form separate from its relationship to other heat transfer mechanisms by measuring the magnitudes of the material electrical resistivity under varying loads.

This paper is devoted to a more detailed study of the regularities of contact heat transfer in powder, fiber sheet, and multilayer systems utilized in cryogenic heat insulation.

We shall first examine the first two groups of materials. Analysis of the data obtained for them is facilitated by the possibility, verified in [2, 3], of utilizing the assumption of additivity of the radiation and conduction in such media.

Dependences of the specific electrical conductivity on the density are presented in Fig. 1 for a number of powder and sheet fibrous materials applied most extensively in vacuum-powder (VPI), vacuum-fiber (VFI), and vacuum-multilayer (VMI) heat insulations.

As is seen from the figure, the dependences mentioned are straight lines in logarithmic coordinates and are approximated by an expression of the form

$$\sigma \sim \rho^k. \tag{1}$$

The values of the exponent k in this formula are given in Table 1 for the materials investigated.

Our data show that the specific electrical conductivity, and therefore, the contact thermal conductivity of pure powders (without metallic admixtures) and of packets of sheet fibrous materials vary in proportion to their density. The addition of metallic admixtures (particularly the bronze powder BPI) shielding the thermal radiation into powder insulation results in noticeable magnification of the dependence of the contact conductivity on the density. Because of the long duration of the experiment, there are practically no such data obtained by the calorimetric method. Only the dependence λ_c—ρ for the mixture aerogel with 45 mass% BPI, shown in Fig. 1 for comparison and approximated by the expression

$$\lambda_c \sim \rho^{4,21}. \tag{2}$$

is presented in [4]. This dependence is in good agreement with an analogous expression for the mixture of aerogel with 40 mass% BPI but its somewhat greater steepness in the first case is due to the elevated content of metallic powder in the mixture.

All-Union Scientific-Research Institute of Helium Engineering, Moscow. Translated from Inzhenerno-Fizicheskii Zhurnal, Vol. 60, No. 1, pp. 121-127, January, 1991. Original article submitted December 27, 1989.

0022-0841/91/6001-0104$12.50